

## Impact of geometric changes in a dilated aorta with a bicuspid aortic valve on blood flow disturbances – a numerical modeling study

Zbigniew Małota<sup>1</sup>, Jan Głowacki<sup>2</sup>, Tomasz Kukulski<sup>3</sup>, Wojciech Sadowski<sup>1</sup>

<sup>1</sup>Fundacja Rozwoju Kardiologii im. prof. Zbigniewa Religi, Zabrze

<sup>2</sup>Pracownia Diagnostyki Obrazowej – TK, Śląskie Centrum Chorób Serca, Zabrze

<sup>3</sup>Śląski Uniwersytet Medyczny, Katedra Kardiologii, Wrodzonych Wad Serca i Elektroterapii, Śląskie Centrum Chorób Serca, Zabrze

Kardiologia i Torakochirurgia Polska 2013; 10 (3): 251–267



### Abstract

Bicuspid aortic valve (BAV) is the most common congenital cardiac malformation that occurs in adults. Bicuspid aortic valve is strongly associated with vascular complications, such as aortic root dilatation, thoracic aortic aneurysms, and aortic dissection. This study attempted to examine the hemodynamic effect of two surgical geometry correction procedures using computer and physical modeling. The estimated changes in basic hemodynamic parameters and the possibility of reducing the risk of aortopathy and valve dysfunction can improve long-term outcomes of BAV patients. The blood flowing through the BAV generates an asymmetric, eccentric, helical flow with a significant secondary flow and increased turbulence area. Asymmetric aortic wall deformation, and the increase and redistribution of stress, may constitute the primary reasons behind endothelial damage and aortic dissection in BAV patients. The surgical correction of the dissipated aortic geometry, in contrast to the separation of the common cusp of the BAV, significantly improves the hemodynamic conditions in the ascending aorta, reduces wall stress, and eliminates the critical point of stagnation on the outer wall of the aorta. *In vitro* modeling methods allow for a patient-specific evaluation of hemodynamic parameters. Two parameters may be particularly helpful in evaluating the degree of aortic dilatation and the risk of aortopathy in BAV patients: the Dean number and the angle between the direction of the main stream flowing out of the valve during the mid-ejection phase and the surface of the outer wall of the aortic arch.

**Key words:** bicuspid aortic valve, hemodynamics, numerical modeling.

### Streszczenie

Dwułatkowa zastawka aortalna (ang. *bicuspid aortic valve* – BAV) to najczęstsza wrodzona wada serca występująca u osób dorosłych. Jest silnie związana z istnieniem wad nabytych aorty wstępującej, takich jak poszerzenie aorty, tętniak aorty oraz jej rozwarstwienie. Obecna wiedza na temat patogenez i następstw występowania BAV pozostaje niepełna. Nie ma przekonujących dowodów na konieczność przeprowadzania prewencyjnych zabiegów plastyki zastawki aortalnej i protezowania aorty wstępującej u chorych bez jawnej hemodynamicznej wady. Niniejsza praca jest próbą przedstawienia zastosowania komputerowych i fizycznych metod modelowania *in vitro* do oceny podstawowych parametrów hemodynamicznych aorty u pacjentów z BAV. Wykorzystując model komputerowy pacjenta z poszerzoną aortą oraz BAV, zamodelowano dwie chirurgiczne procedury naprawcze, które pozwolą na uzyskanie odpowiedzi, czy zmiana geometrii aorty lub rozcięcie wspólnego płatków BAV może wpłynąć na poprawę warunków hemodynamicznych w aorcie. Przepływ krwi przez BAV generuje w aorcie asymetryczny, spiralny przepływ, ze znacznym przepływem wtórnym i ze zwiększonym obszarem turbulencji. Asymetryczna deformacja ściany aorty, wzrost i redystrybucja naprężeń może stanowić podstawową przyczynę uszkodzenia śródbłonna i rozwarstwienia aorty u pacjentów z BAV. Chirurgiczna zmiana geometrii poszerzonej aorty istotnie poprawia warunki hemodynamiczne w aorcie wstępującej i likwiduje krytyczny obszar stagnacji na zewnętrznej ścianie aorty wstępującej. Dwa parametry – kąt natarcia pomiędzy kierunkiem głównego strumienia wypływającego z zastawki podczas środkowej fazy wyrzutowej a powierzchnią zewnętrznej ściany łuku aorty oraz liczba Deana – mogą być użyteczne w określeniu stopnia poszerzenia aorty i ryzyka wystąpienia aortopatii u osób z BAV.

**Słowa kluczowe:** dwułatkowa zastawka aortalna, modelowanie numeryczne, hemodynamika.

**Address for correspondence:** Zbigniew Małota, Fundacja Rozwoju Kardiologii, ul. Wolności 345a, 41-800 Zabrze, phone: +48 32 373 56 26, e-mail: zmalota@frk.pl

## Introduction

Bicuspid aortic valve (BAV) is the most common congenital heart defect, occurring in as much as 1-3% of the adult population. In most cases, the valve initially functions normally, without any clinical symptoms. Only after many years of life do the complications and defects present themselves; they are significantly more frequent in the case of BAV than in the case of a normal tricuspid aortic valve (TAV). For example the risk of aortic dissection is only 0.67% for persons with a tricuspid valve, while the same risk for persons with BAV is over 6% [1].

Due to the frequent coexistence of other congenital defects, determining the impact of BAV on the said congenital defects is very difficult. The link between BAV dysfunction and aneurysms, dissections, and dilatations of the aortic trunk, as well as endocarditis, has been known for many years [2-7]. In 1928, Abbott and Hamilton [2] noted the coexistence of BAV with aortic coarctation and dissection. McKusick *et al.* [5] postulated a hypothesis concerning the interactions between hemodynamic properties in BAV patients with concomitant ascending aortic dissection and the necrosis of aortic muscle tissue. Pachulski and Weinberg [6] and Bonderman *et al.* [3] observed that large aortic trunk diameters are more frequent among patients with BAV than among patients with normal aortic valves. Hahn *et al.* [4] demonstrated that the largest aortic dilatations occur in patients with significant valvular regurgitation. In turn, histochemical studies demonstrated increased apoptosis of aortic smooth muscle cells in patients with BAV [7]. It was observed that BAV is always accompanied by structural changes in the aorta, including its decreased elasticity resulting from the disruption of the collagen-elastin structure, smooth muscle atrophy, and decreased fibrillin-1 and microfibrillar production [7]. Disorders of vascular connective tissue, such as the loss of elastic tissue, may lead to the dilatation of the aortic bulb or the ascending aorta. Decreased elasticity of the aortic wall results in its greater stiffness (greater Young's modulus) and increases the systolic arterial pressure and heart rate amplitude. Strong blood flow (flow turbulence) may also cause structural changes of both the endocardium (during diastole, due to BAV insufficiency) and the aortic endothelium cells (during systole, due to significant BAV stenosis) [8].

Interactions between the hemodynamic parameters of BAV and ascending aortic dissection, aortic smooth muscle necrosis, increased aortic trunk diameter [3, 6], and regurgitation [4] have also been hypothesized [5]. Robiscek *et al.* [9] hypothesized that high stress values may result in early BAV cusp thinning, as well as valve calcification and stenosis, and that a change of BAV hemodynamic properties may influence the dilatation of the ascending aorta. They also observed a significant impact of cusp plication on the dynamics of valve opening. Hope *et al.* [10] used four-dimensional flow MR imaging for the evaluation of aortic blood flow. They demonstrated the existence of helical flow in the ascending aorta at systole in BAV patients who did not suffer from aneurysms or aortic stenosis.

They noted that the identification and characterization of eccentric blood flow jets in these patients may facilitate the evaluation of the risk of aortic aneurysm development. However, the current state of knowledge concerning the pathogenesis and consequences of aortic defects is still insufficient (in part due to the influence of hemodynamic disturbances). Taking into consideration the pronounced heterogeneity of the BAV defect, further research is required in order to verify the validity of the postulated hypotheses. At the moment, there is no theoretical model explaining the influence of BAV on the abovementioned defects, that would allow for a quantitative estimation of the likelihood and extent of their occurrence. Girdauskas *et al.* [11] stated that right-left-coronary-cusp fusion in BAV (RL BAV) is clearly associated with aortic trunk dilatation, while right-non-coronary-cusp fusion (RN BAV) is related to isolated dilatation of the ascending aorta (without aortic trunk dilatation). In their view, this relationship between BAV morphology and the distribution of aortic dilatation confirms the hemodynamic link between BAV and aortopathy. Contrarily, based on the lack of correlation between the degree of BAV stenosis and the size of aortic dilatation, Wilton *et al.* [12] came to the conclusion that aortic dysfunction results more from aortic pathologies than from hemodynamic effects and aortic valve dysfunctions.

Therefore, the question remains, to what extent the dysfunction of an initially normally functioning BAV is attributable to genetic changes, and to what extent it results from hemodynamic changes [11]. Due to the frequent coexistence of other congenital defects, determining the impact of BAV on the abovementioned congenital defects is very difficult. The influence of BAV dysfunction on aortic defects is also related to age. The later BAV stenosis occurs, the greater is the likelihood that serious hemodynamic changes will not develop before the age of 70.

Concurrently, the possibility of performing an early surgical repair of the bicuspid valve may significantly facilitate the efficacy of treatment and reduce the risk of long-term complications that present only after many years of life. There is currently no convincing evidence with regard to the necessity of performing preventive aortic valvuloplasty and ascending aortic grafting in patients with no overt hemodynamic defects.

The incidence of other congenital defects, which frequently occur jointly with BAV, may suggest that the development of this type of valve is caused by genetic factors. This is partially confirmed by studies on heredity in first-degree relatives [13]. Bicuspid aortic valve is 4 times more common among men than among women.

In most patients (92%), the BAV cusps differ in size, as two cusps are fused into one dominant cusp. The line of cusp coaptation (the so-called raphe) is more often observed on the anterior cusp and stretches from the cusp's rim all the way to its base.

Aortic valve stenosis is the most common consequence of BAV. In over 50% of adults with aortic valve stenosis, the origin of the disease is related to a bicuspid aortic

valve. However, most BAV patients without any signs of stenosis during their youth experience gradual premature valve degeneration.

Sabet *et al.* [14] demonstrated the presence of stenosis in as many as 85% of patients diagnosed with BAV. The reason why valve stenosis occurs more frequently in BAV patients than in patients with tricuspid aortic valves has not yet been discovered. In the case of BAV, it is thought that the reason behind the faster degeneration of valve cusps is the excessive stress to which both cusps are exposed, along with turbulent aortic blood flow. Patients with BAV and signs of stenosis require periodic echocardiographic monitoring in order to evaluate the progression of the defect and the width of the ascending aorta. The qualification criteria for valve replacement are identical to those concerning stenoses of other etiology; the surgery may be expedited if the ascending aorta dilates to more than 4.5 cm [4, 12].

Significant aortic valve insufficiency is much less common, occurring in only 15% of patients with diagnosed BAV [15]. The insufficiency is related to the dilatation of the cusps' attachment site, which results in incomplete cusp coaptation and may facilitate cusp prolapse. The insufficiency may also be a result of previous aortic valve endocarditis. Endocarditis is a potentially destructive complication, which occurs in approximately 30% of BAV patients, particularly among younger patients with valvular insufficiency [8]. It should, however, be stressed that a slight insufficiency in the vicinity of the valve commissures is present in most BAV patients [11, 13].

Bicuspid aortic valve is an independent risk factor for the gradual dilatation of the aorta. It has been demonstrated that the dilatation of the lumen of the ascending aorta is caused by progressive and premature degenerative changes of the middle layer of the aortic wall. This results in the weakening of the aortic wall, which may cause the development of an aneurysm, or even aortic wall dissection. Young men constitute the group that is most susceptible to acute dissection; therefore, regular echocardiographic evaluation of the aortic width is recommended for BAV patients. Aortic dissection is the most dangerous complication of BAV. In an evaluation of the clinical condition of 1407 BAV patients, aortic dissection was revealed in 35 cases (2.5%) and was most often concomitant with aortic insufficiency [12]. Aortic wall rupture at the dilated sinuses of Valsalva can also sometimes be observed.

Recent scientific studies have provided more insight into the genetics, pathobiology, and clinical progression of the disease, but there are still questions to be answered. The work by Siu *et al.* [1] has summed up the current state of research with regard to the pathology, genetics, and clinical aspects of BAV disease, focusing on the BAV pathologies in the adult population. The authors underline that only full comprehension of the degenerative process of BAV and aortic dilatation can enable the development of new, more efficacious therapeutic protocols. Valve stenosis and susceptibility to early fibrosis, stiffening, and calcification of cusps can be observed in most BAV patients

between the ages of 15 and 65. The anatomy of BAV may also influence the development of an arterial embolism. Stenosis progresses faster in the case of asymmetric cusps or the antero-posterior position.

Vascular complications associated with BAV are less understood than the complications of the valve itself, and they result in greater mortality. It is believed that vascular defects in BAV patients are not secondary to valve dysfunction and can often present without significant stenosis in younger patients in whom the natural BAV valve was replaced with a prosthesis.

In fact, as many as 50% of young patients with BAV present with aortic dilatation, which may later result in aortic rupture and dissection.

Making correct decisions regarding the surgical repair of BAV requires the BAV patients to be constantly monitored. The currently performed procedures for aortic dilatation with BAV may consist in [16]:

- replacing only the dilated part of the aorta above the sinotubular junction with a prosthesis (most often made of Dacron) without removing the natural valve,
- replacing the dilated part of the aorta and performing valvuloplasty or replacement of the bicuspid valve with a prosthesis,
- or replacing the dilated part of the aorta which may include the aortic trunk and sinuses.

In recent years, the view that valvuloplasty is the best method of treating BAV defects has gained more acceptance. An analysis of patients treated with various methods [17] indicated that BAV insufficiency repair is most efficacious in patients with non-coaxial retrograde flow, without cusp thinning or calcification.

Numerical modeling methods are an effective tool for analyzing blood flow in the circulatory system and evaluating the system's hemodynamic changes resulting from the planned procedure [18, 19]. Significant improvements have been made in recent years with regard to numerical simulations of blood flow through cardiac valves. Notwithstanding, only a few scientific reports, such as Robiscek *et al.* [9] and Weinberg *et al.* [20], were directly concerned with computer modeling of blood flow through bicuspid aortic valves. Only Chandrain *et al.* [21] presented initial reports of using the FSI method (fluid-structure interaction), taking into consideration the wall-fluid interaction in order to determine the potential consequences of mechanical stress in a simple model of an aortic trunk with a bicuspid aortic valve. The conducted literature review revealed no reports concerning the modeling of repair procedures for ascending aortic dilatation in BAV patients.

### Aim of the study

The aim of the present study was to employ the FSI method in order to evaluate the degree to which geometric changes of a dilated aorta influence the flow distribution and basic hemodynamic parameters in patients with BAV.

Using a computer model of a patient with a dilated aorta and RL BAV, two repair procedures were modeled, that

will allow one to assess whether changing the aortic geometry or separating the fused BAV cusp may produce an improvement of the hemodynamic conditions in the aorta.

The computer model, prepared on the basis of clinical studies and patient-specific imaging techniques, may be helpful in selecting appropriate treatment methods in dependence on the hemodynamic conditions in the circulatory system and the mechanical properties of the aortic wall, thus reducing the probability of the occurrence of BAV dysfunction or defects of the ascending aorta, and, consequently, improving long-term treatment outcomes.

## Methodology of experimental and numerical research

Modeling the functioning of a cardiac valve should include both a blood flow analysis and an evaluation of the movement dynamics of the valve cusps. The aorta and the valve cusps are built from a material of complex structure and viscoelastic, anisotropic, and non-linear mechanical properties [22]; therefore, in order to obtain the whole picture of the functioning dynamics of the valve, a model with movable, elastic walls (with specified mechanical properties), taking into account the fluid-structure interaction (FSI), was used. Employing such a model enables the analysis of interactions between blood flow characteristics (with specified rheological properties) and the mechanical properties of the aorta and the valve. Figure 1 presents the simplified *in vitro* modeling scheme that was used in the research project.

The study method is based on clinical data. Medical imaging constitutes the basis on which physical and computer models are constructed. Clinical data were obtained from routine examinations of patients with bicuspid aortic

valves conducted at the Silesian Center for Heart Diseases in Zabrze. Computer and physical models of the aorta and the valves were prepared based on the CT images of a patient with the most frequent phenotype of BAV (10), i.e., with a single raphe between the fused coronary cusps (R-L).

Reconstructing the 3D structure of the aortic models was based on the process of segmenting a set of 2D images obtained from CT, archived in a DICOM format with the resolution of 512 x 512 pixels. The 3D model reconstruction was performed using the 3D-DOCTOR software package (Fig. 3), developed by Able Software Corp., and Rhinoceros® (Robert McNeel & Associates). 3D-DOCTOR enables the performance of interactive segmentation by specifying the threshold values of specified regions of interest (ROI). In order to create 3D surfaces based on the marked contours of selected objects, a fast vector-based algorithm is applied to all planes. The Rhinoceros® software creates NURBS geometry and enables the modification of a geometry based on polygons and point sets. A ready three-dimensional model of the aorta in CAD format constitutes a basis for the generation of a 3D grid of finite elements, required for the simulation of computational fluid dynamics (CFD) based on the finite elements method (FEM). The physical model of the aorta (Fig. 4A) was constructed by means of rapid prototyping using PolyJet technology (BibusMenos.pl). The material employed in the project was Tango Plus FullCure 930 (Object Ltd.) – an elastic material of milky color, Shore hardness of 27 (A scale), tensile strength of 1.5 MPa, and elasticity coefficient of 0.1 MPa.

The aortic bicuspid valves (Fig. 4B) used for experiments at the physical research station were made from VytaFlex – polyurethane rubber – using a direct casting method. Valve forms were made of ABS (acrylonitrile-butadiene-styrene) materials by means of rapid prototyping using fused deposition modeling (FDM) technology. The blueprint for the form and models was created using Autodesk Inventor software.

The Newtonian model of fluids, in which shear stress  $\tau$  is a linear function of the deformation speed tensor, was used along with the shear stress transport (SST) flow turbulence model – a model which is averaged with regard to time and based on  $\kappa$ - $\epsilon$  and  $\kappa$ - $\omega$  models [23]. This model can also be applied in the case of turbulence with low Re value and in flow separation regions (vicinity of valve cusps, vascular divisions); hence its use in, e.g., aortic blood flow simulations [24]. Based on our own durability studies, computer models of the geometry of an aorta with elastic walls and mobile valve cusps were prepared. An orthotropic valve cusp model was assumed, with a longitudinal elasticity module of 2 MPa and a peripheral module of 12 MPa. An isotropic model was assumed for the aorta, with an elasticity module of 1.7 MPa. Due to the complexity of the model's geometry, a four-sided numerical FEM grid was used, with a finer grid in the vicinity of the valve cusps. The numerical grid of the fluid area contained approximately 800,000 elements, whereas that of the aortic walls contained approxi-

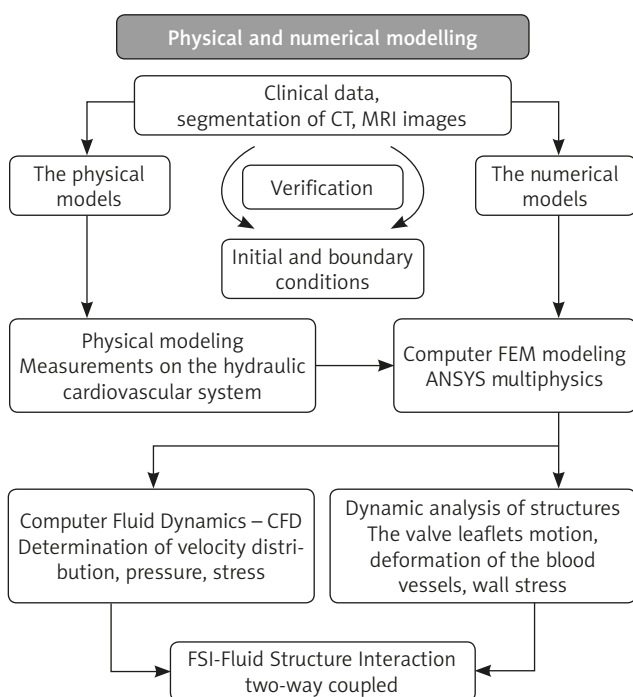
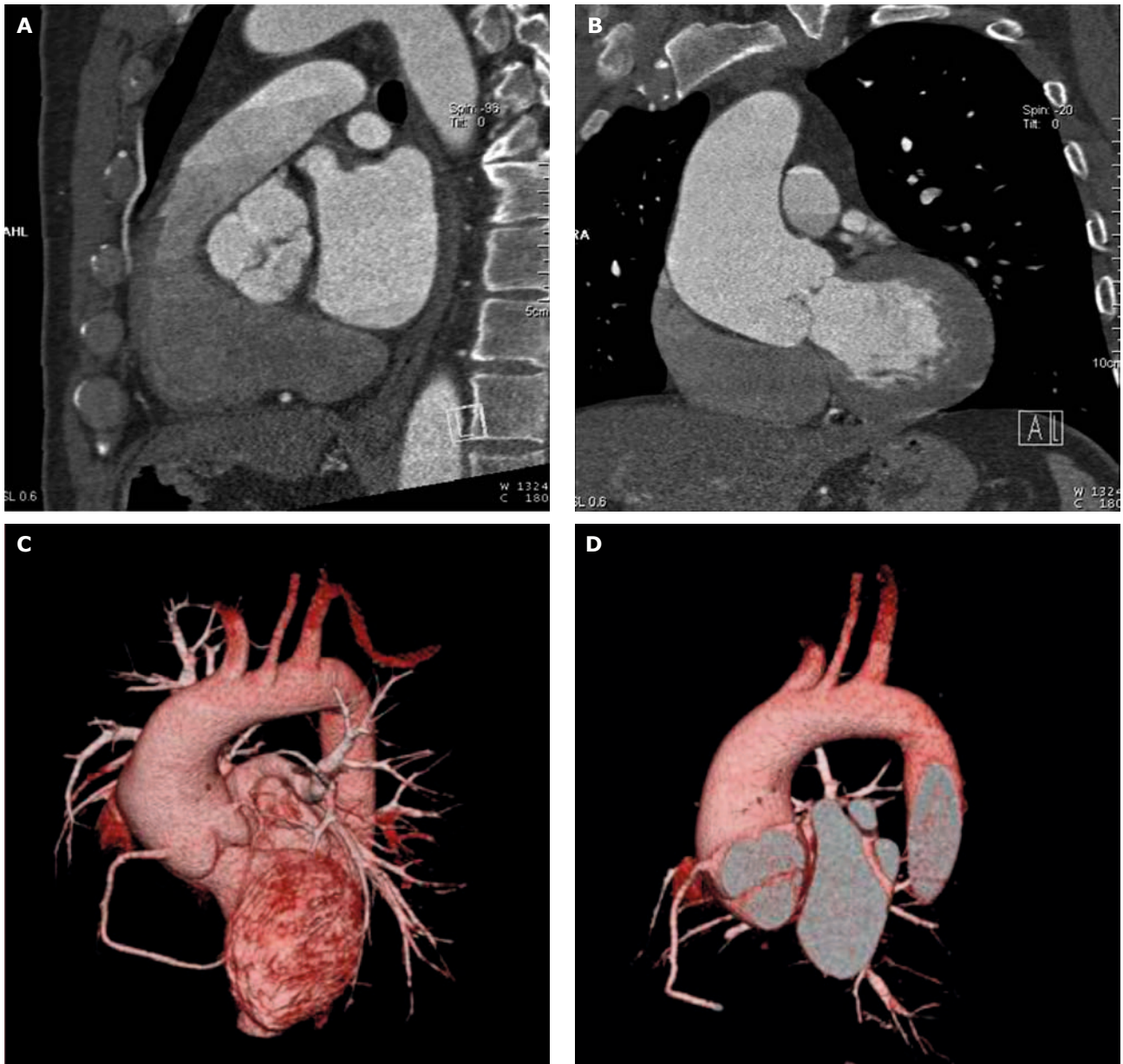


Fig. 1. A general scheme of circulatory system modeling



**Fig. 2A-D.** An example of clinical data of a patient with BAV: A, B) single CT images in two different planes of projection, C, D) 3D volume rendering

mately 50,000. Computer simulations were conducted for identical threshold and initial conditions. At the aortic inlet, a flow rate curve was set (with a mean rate of 4.5 l/min), which had been obtained during experiments conducted on the hydraulic circulatory system. Vascular resistance was specified at the outlets of all of the model's branches (model 1) in order to achieve physiological flow rate distribution. The proportions of blood flow from the aorta to the arteries were set in the following manner:

- 10% for the right common carotid artery (RCCA),
- 7.5% for the left carotid artery (LCA),
- 2.5% for the left subclavian artery (LSA),
- and approximately 5% for the coronary vessels.

For the purposes of the project, two procedures were selected for the repair of the dilated aorta with BAV.

The first consisted in the replacement of the dilated part of the aorta according to the scheme presented in Figure 5C. The second method involved a simulation of the influence of separating the fused cusps on the basic hemodynamic parameters (Fig. 5D).

The following computer models of patients were created:

1. Model 1 (Fig. 5A) – a model of an aorta with a normal tricuspid aortic valve, prepared on the basis of angio-CT imaging of coronary arteries in a 40-year-old female patient, conducted due to complaints of unspecified chest pains and a suspicion of coronary disease. The examination ruled out coronary artery changes; the dimensions of the thoracic aorta were normal. The aorta and the tricuspid aortic valve had normal structure.

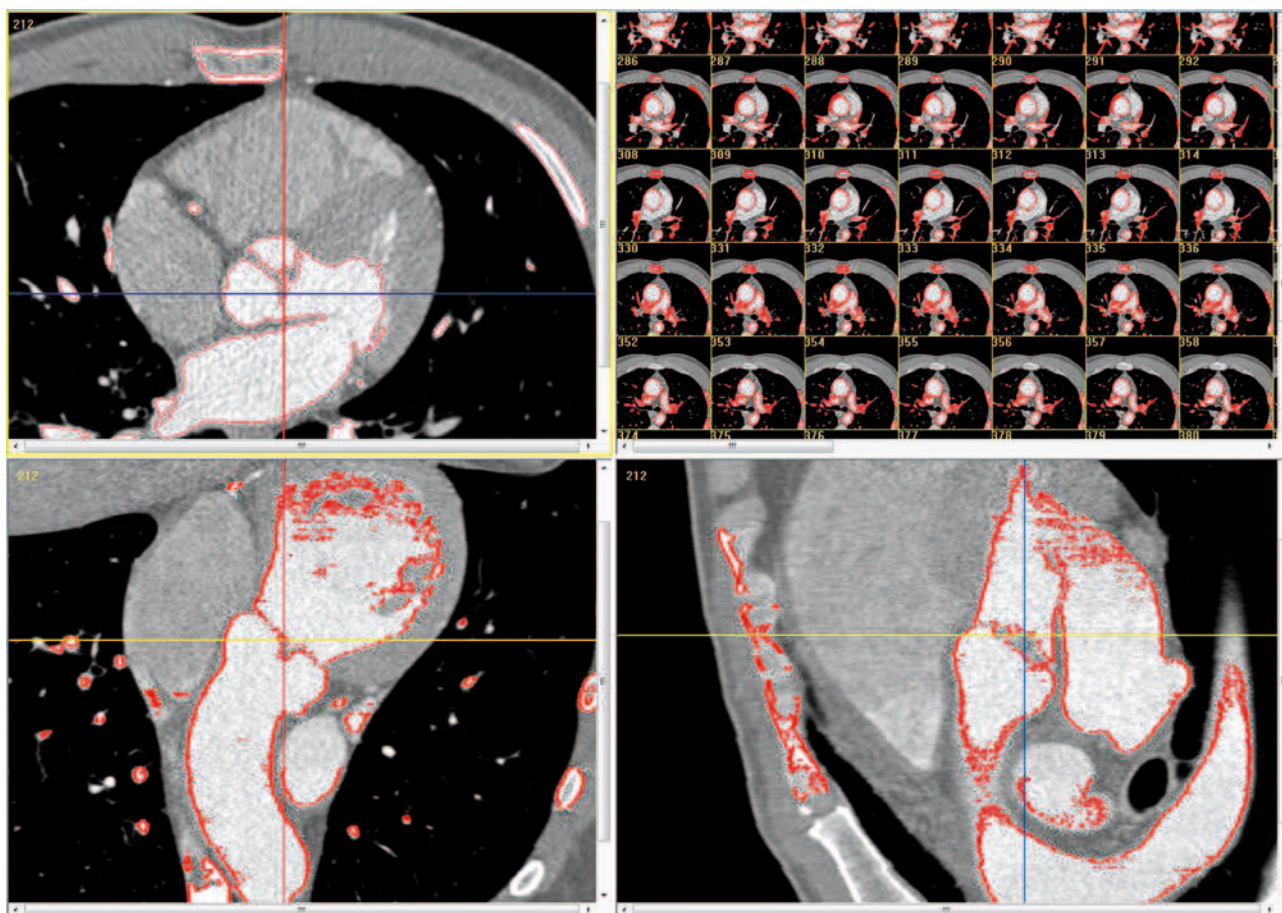


Fig. 3. CT image segmentation; ROI (regions of interest) marked in 3D-DOCTOR software (Able Software Corp.)

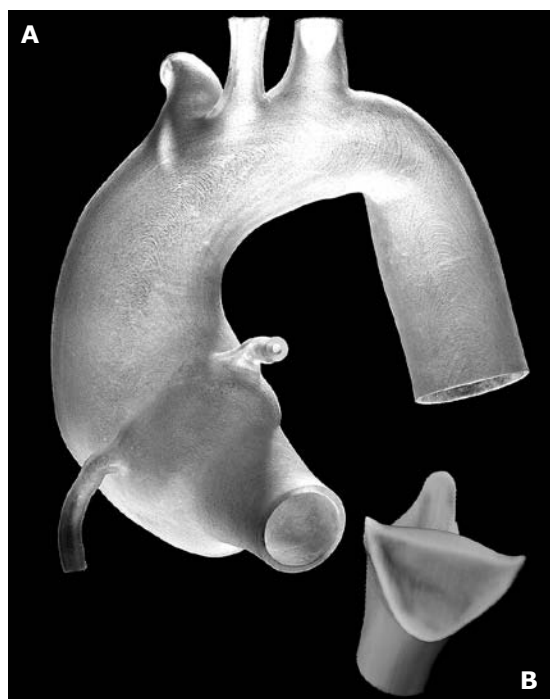


Fig. 4A-B. An example of an elastic model of an aorta with BAV (made of FullCure 930 material), which was used for testing at the hydraulic circulatory system station

2. Model 2 (Fig. 5B) – a model of a dilated aorta with RL BAV, prepared on the basis of angio-CT imaging of a 53-year-old male patient, referred for examination on suspicion of an aneurysm of the ascending aorta, diagnosed based on chest scans and ECG examinations. Angio-CT revealed the presence of an ascending aortic aneurysm with maximum dimensions of  $5.8 \times 5.2$  cm. The remaining aortic dimensions were as follows: annulus – 2.9 cm, bulb – 4.3 cm, sinotubular junction (STJ) – 4.6 cm, aortic arch – 2.5 cm. The examination did not reveal any signs of aortic dissection; it did, however, reveal the presence of a bicuspid aortic valve.

Based on model 2, two additional models were created:

3. Model 3 (Fig. 5C) – a model of an aorta with RL BAV, in which the dilated part of the ascending aorta was replaced with a patch.

4. Model 4 (Fig. 5D) – a model of an aorta with RL BAV, in which the fused RL cusp was separated, thus forming a new aortic valve with three separate cusps.

In order to verify the numerical calculations and determine the correct selection of a solver in the ANSYS Multiphysics software, the simulation results were compared with the experimental data obtained from measurements conducted on a simple hydraulic circulatory system. The circulatory system measurement station was based on

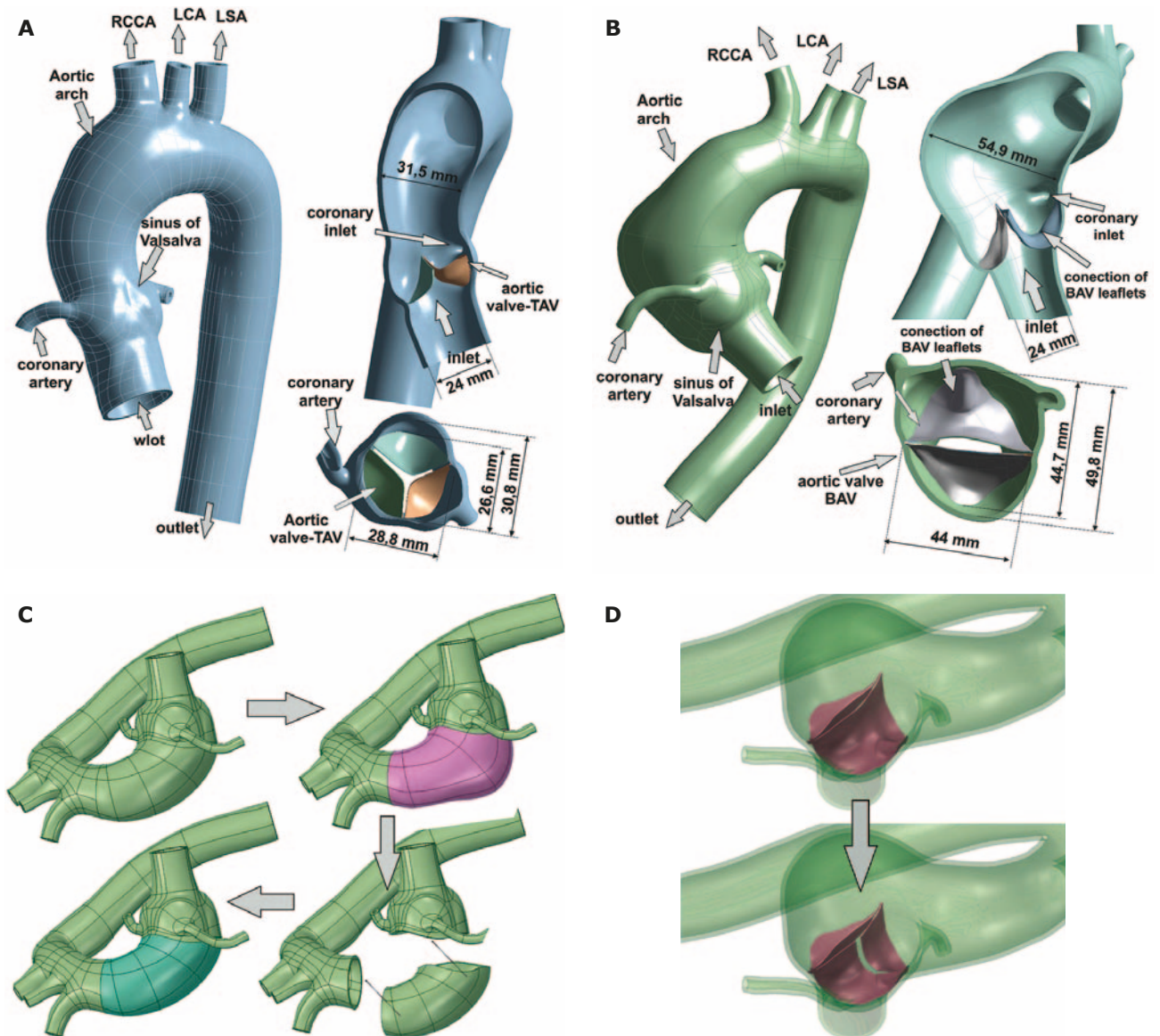


**Fig. 5A-D.** 3D computer aortic models: A) model 1 – a model of a normal aorta with TAV, constructed on the basis of CT images of a 40-year-old female patient, B) model 2 – a model of a dilated aorta, constructed on the basis of CT images of a 65-year-old male patient with BAV, C) model 3 – a model of an aorta with RL BAV, in which the dilated part of the ascending aorta was replaced with a vascular prosthesis, D) model 4 – a model of an aorta with RL BAV, in which the fused RL cusp was separated, thus forming a new aortic valve with three separate cusps

the Windkessel effect [25] (Fig. 6). A POLVAD ventricular assist device, with a JSN-301 driving unit, was applied in the system. A high-pressure low-volume potential energy reservoir served the role of the arterial system. A 40% water-glycerol solution, with a viscosity of 3.4 centipoise and a density of  $1.04 \text{ g/cm}^3$ , was used as the blood analogue. Adequate circulatory conditions were achieved by changing the control parameters of the POLVAD ventricle (frequency, suction pressure, forcing pressure, systolic filling fraction) and setting appropriate resistance and susceptibility in individual branches of the system.

The basic criteria of flow similarity require the model and the physical object to share kinematic, dynamic, and geometric flow similarity. The main criterion of similar-

ity of viscous fluid flow in a blood vessel, resulting from the use of Navier-Stokes (N-S) equations [26], is the Reynolds criterion (of viscosity force similarity), which requires the geometric similarity of bounding surfaces and equality of the Re number. This number expresses the ratio between the forces of inertia and viscosity, and it constitutes a measure of flow turbulence. In the case of small Reynolds numbers, the forces of viscosity play a decisive role in the flow, suppressing all disturbances and making the flow laminar. An increase in the Reynolds number resulting from increasing velocity causes a rise in the force of inertia, proportional to the square of velocity, and an increase in the force of viscosity that is proportional to velocity. Therefore, the larger the Re number, the bigger is the role in flow

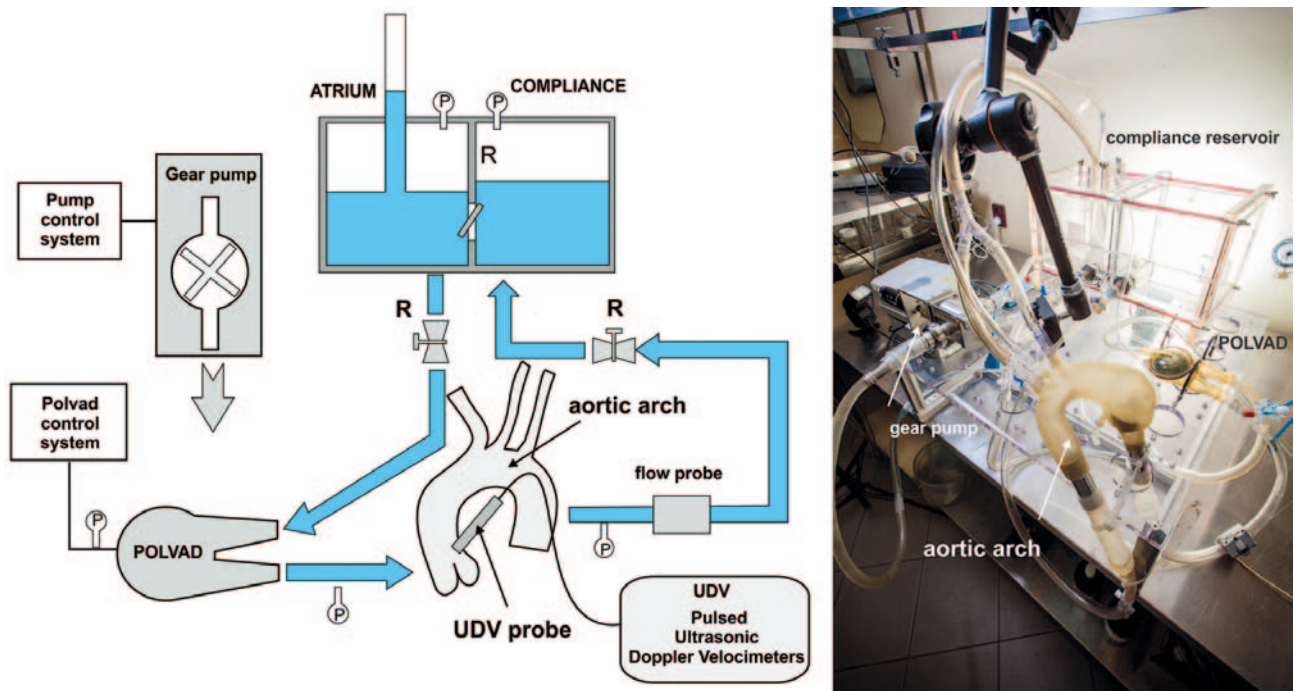


Fig. 6. A scheme of the measurement station used for evaluating blood flow through aortas with TAV and BAV

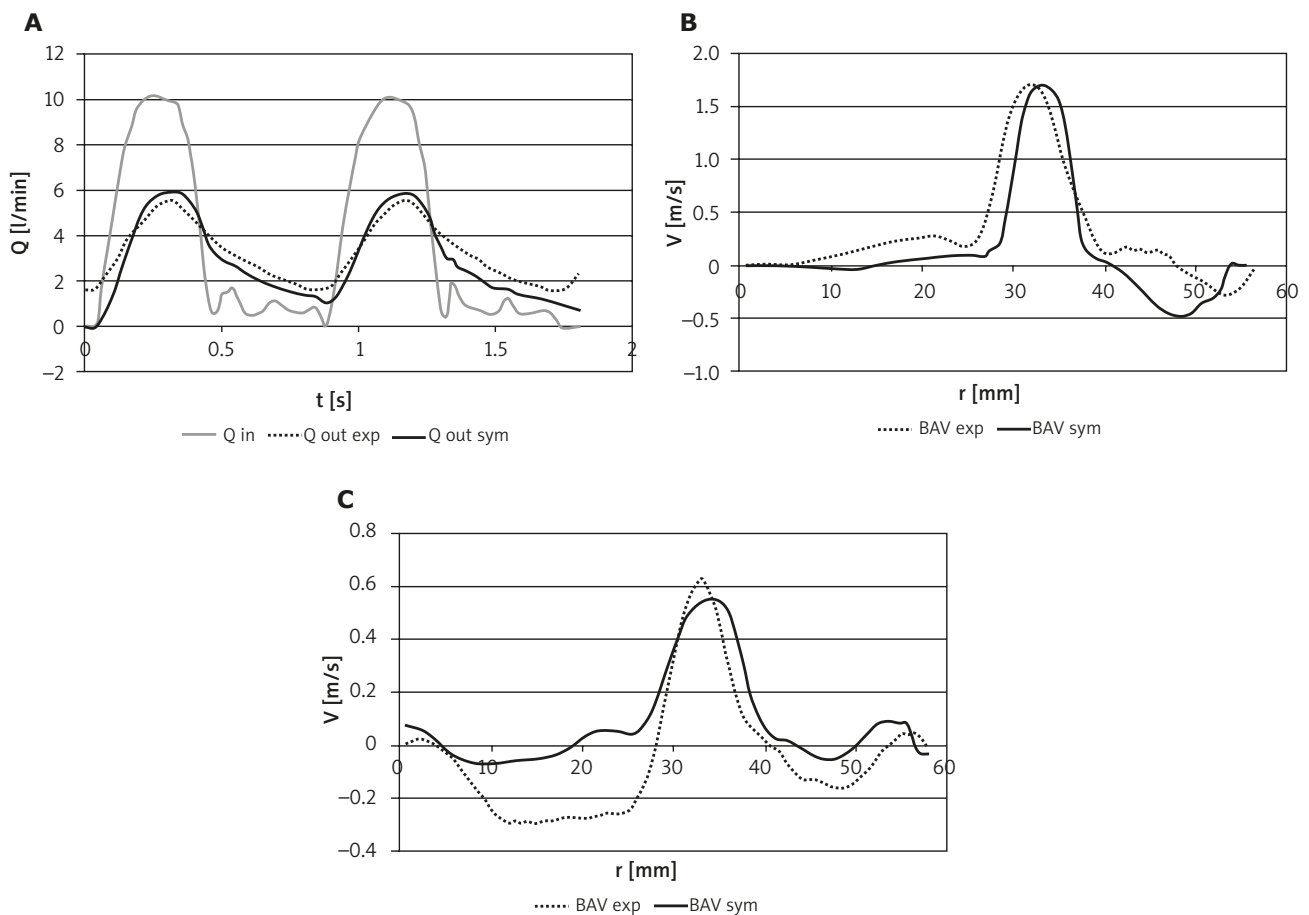


Fig. 7A-C. A comparison between computer simulation results and experimental data obtained using the hydraulic circulatory system: A) aortic flow rate, B) velocity profiles during early systole, C) velocity profiles at mid-systole



played by the forces of inertia. After reaching a specified critical value of the Reynolds number, laminar flow transitions into turbulent flow. In the case of undetermined flow, the Strouhal number should be considered along with the Reynolds number. At the aortic inlets of all models, the mean Re number was approximately 1410, while the Strouhal number was approximately 0.026.

Measurements of pressure, flow rate, and velocity profiles were taken at the hydraulic station (Fig. 6). The flow rate measurements were taken in individual branches of the model with a Transonic System ultrasonic flowmeter with a measurement precision of  $\pm 5\%$ . Pressure measurement was conducted with typical medical detectors with a measurement precision of  $\pm 2\%$ .

The velocity profiles were measured with a pulsed ultrasonic Doppler velocimeter – DOP2000 (Signal Processing SA). In contrast to regular ultrasonic flowmeters, this device enables the simultaneous measurement of instantane-

ous local velocities in multiple locations. The velocity profile measurement was taken in two perpendicular planes, located at the distance of 25 mm and 45 mm from the point of valve insertion.

The conducted validation revealed good conformity between the computer simulation outcomes and the experimental data (Fig. 7). In the case of flow rate and pressure values, the difference was smaller than 5% in all branches of the model. The increased deviation in the early systolic phase was primarily a result of a measurement error: in the vicinity of the model's wall, the ultrasonic signals of the Doppler impulse flowmeter overlapped as they were reflected by the moving boundaries of the medium (wall, mobile cusps).

## Results and discussion

The shape of the boundary layer is of fundamental importance with regard to calculating resistance during

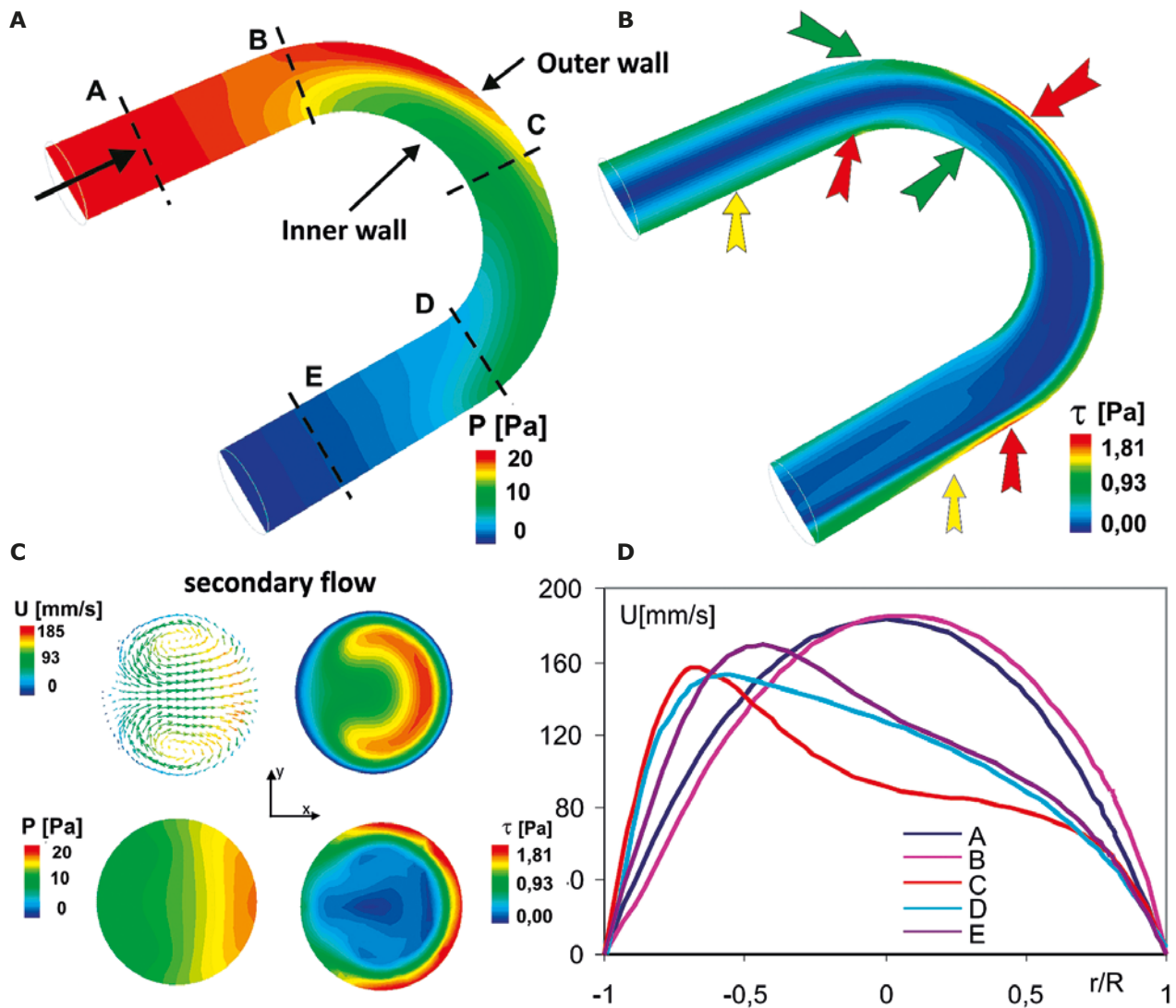


Fig. 8A-D. A computer simulation of blood flow through a vascular arch: A) pressure distribution [Pa], B) shear stress distribution [Pa], C) vectors of velocity, distribution of velocities, pressure, and shear stresses in a section transverse to the axis of the vessel, D) velocity profiles obtained from computer simulation of various sites of the vessel arch (in a plane crossing the vessel axis)

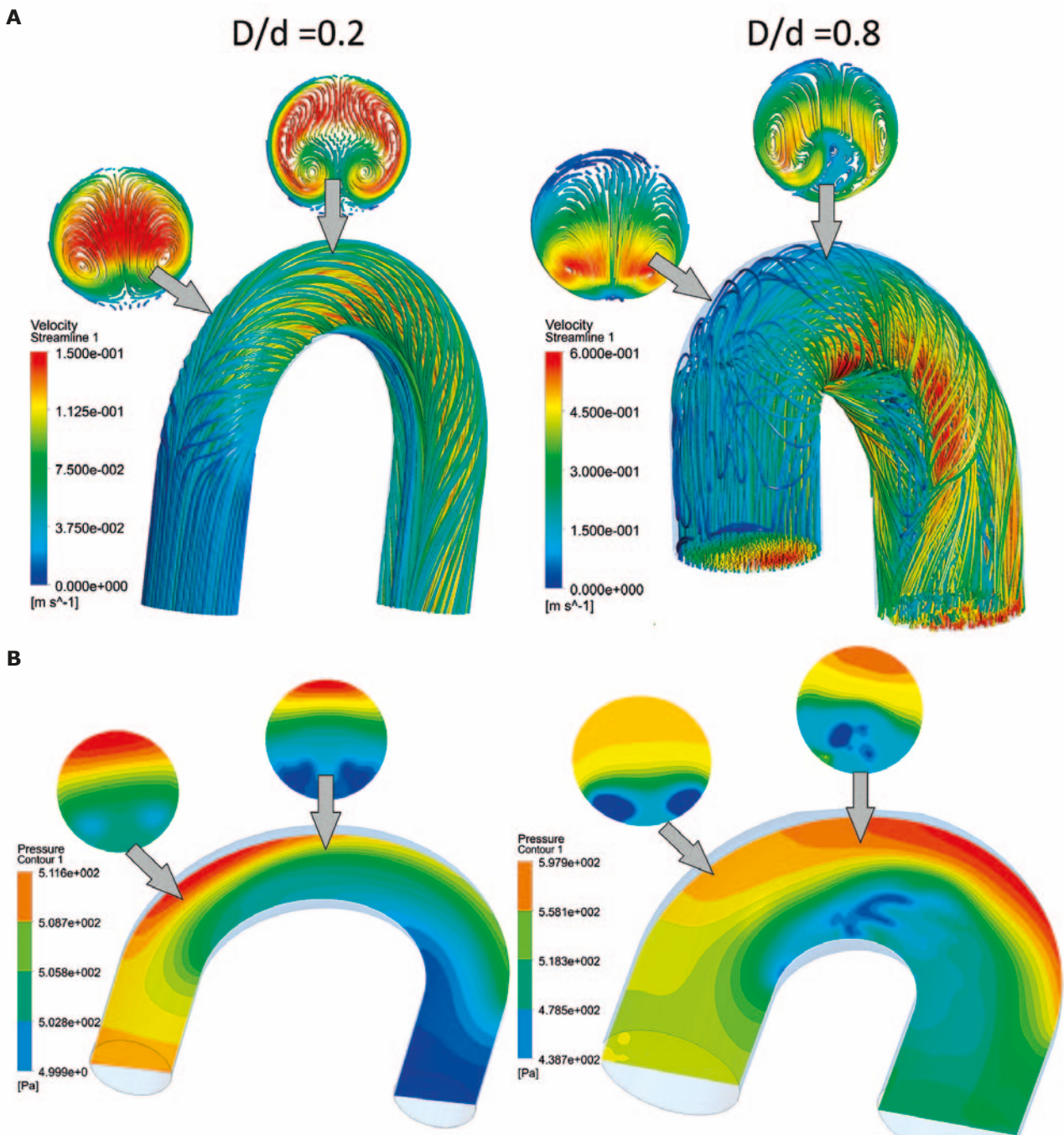


Fig. 9A-B. The influence of vessel arch curvature ( $D/2r$  ratio) on: A) secondary flow and flow disturbances, B) pressure distribution

the movement of the fluid. At the margin of the boundary layer, viscosity forces are comparable to the forces of inertia. When the pressure gradient is negative ( $\partial p/\partial x < 0$ ), the velocity in the direction of the flow ( $x$ ) increases, and the velocity profile is a convex curve; when the gradient is a positive number ( $\partial p/\partial x > 0$ ), the velocity in the direction of the flow is reduced, which may cause retrograde flow (swirling, stream separation). A point of inflection appears with a condition of stream separation ( $\partial^2 u_x/\partial y^2 = 0$ ). Stream separation occurs when the kinetic energy of the fluid in the vicinity of the wall drops to zero.

The blood flow in the aortic arch is made even more complex by the fact that the movement of particles in the vessel is not parallel to the curved flow axis. The free stream (approximately non-viscous) is well described by the Bernoulli equation [25]. Particles traveling along an arch experience centrifugal acceleration (in the direction normal to the flow), equilibrated locally for each particle with the pressure gradient equal to  $2\rho u^2/d$  ( $d$  – arch diameter). The pressure rises from the middle of the arch in the outward radial direction. The pressure differences are equilibrated by centrifugal forces. According to the Ber-

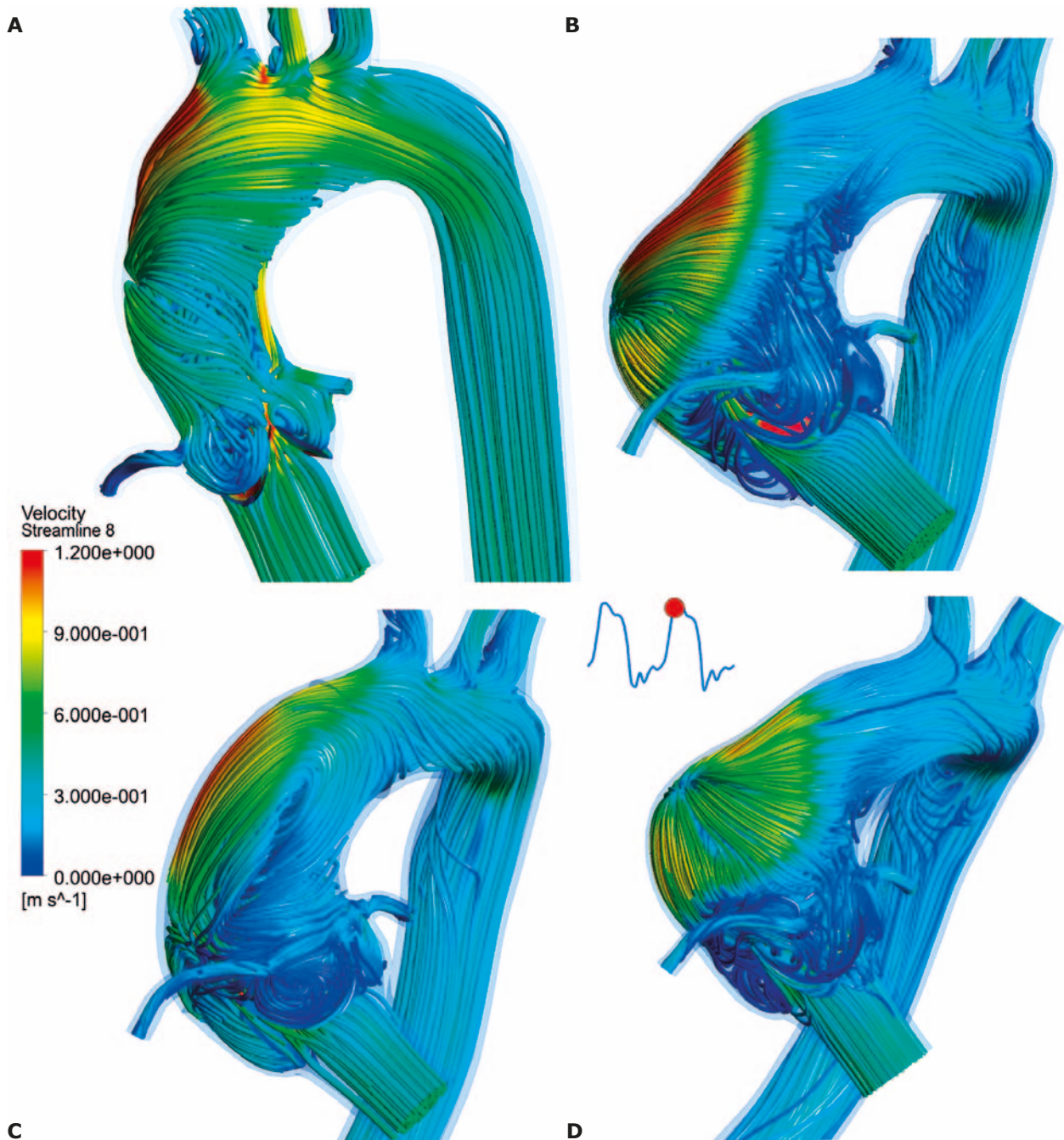


Fig. 10A-D. The spatial distribution of the lines of flow at mid-systole for selected models

no null equation, the velocities on the inner wall of the arch will be higher than on the outer wall. In turn, due to the influence of viscosity forces, velocity is much lower near the walls than in the axis of the circuit; therefore the radius of the trajectory curve is larger in the free stream than in the boundary layer, and the fluid is pushed in the outward direction (in boundary layers, the flow velocities are reduced to zero and the centrifugal forces cannot equilibrate the pressure difference). Thus, a secondary flow develops transversely to the axis of the vessel and influences the distribution of longitudinal velocity (Figure 8); the flow

stream in the arch is spiral. The shorter the arch radius or the higher the flow velocities (at the inlet), the more twisted the flow helices (the helical pitch is shorter) and the larger the loss of kinetic energy. The nature of flow in a curved vessel is well described by the Dean number:

$$De = Re \sqrt{\frac{D}{2r}},$$

which expresses the relation between viscosity and inertia forces in dependence on pipe diameter  $D$  and curve radius  $r$  [27].

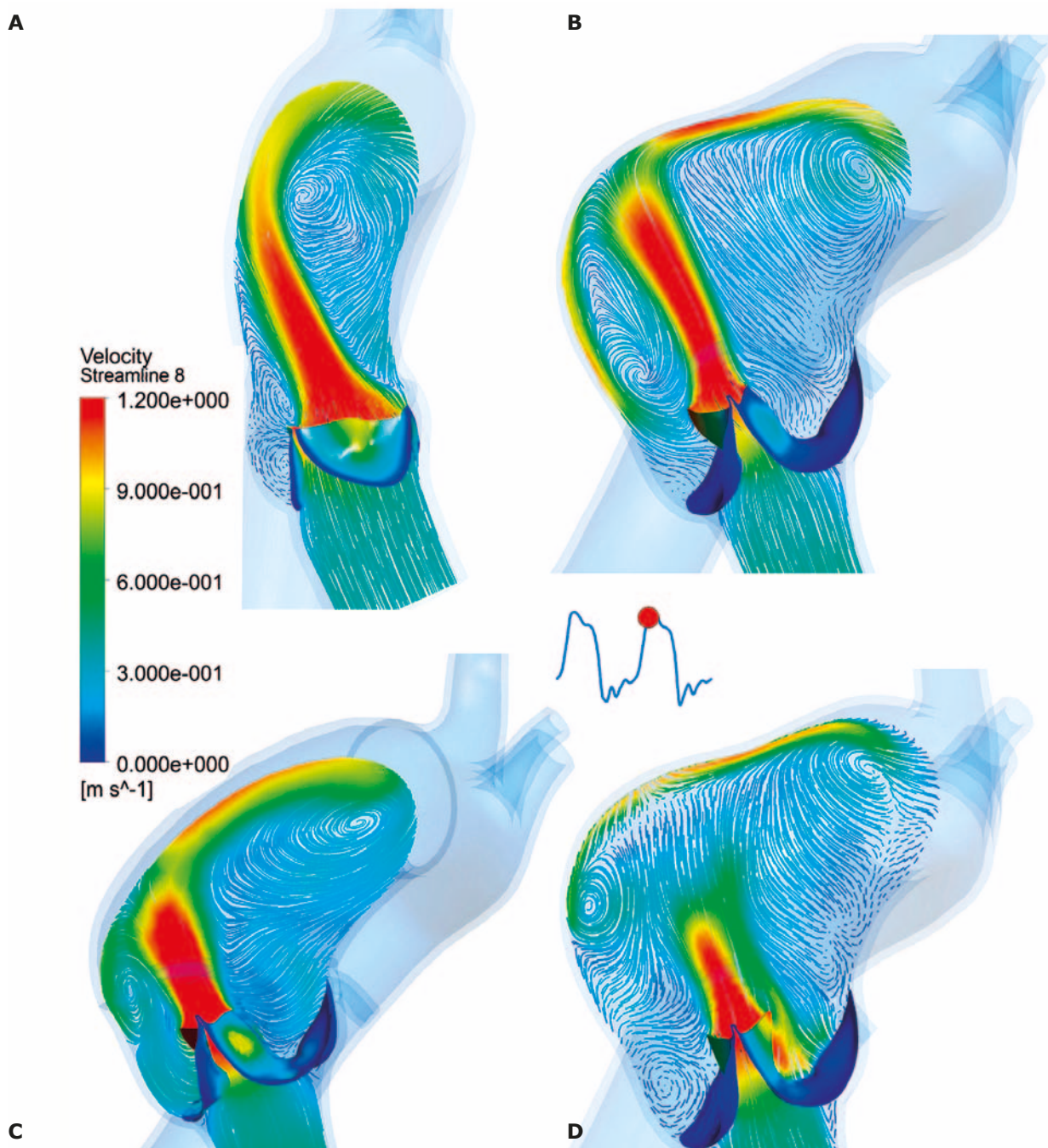


Fig. 11A-D. Lines of flow visualizing blood flow at mid-systole in a plane crossing the middle of the valve along the aortic axis

As the Dean number rises, the single secondary flow transitions into a double flow. If the radius of the vessel arch is too short (high  $D/2r$  ratio), stream separation points appear, increasing local flow loss (Fig. 9). In turn, if the curve is mild (low  $D/2r$  ratio), stream separation does not occur, but flow loss rises due to friction, because of the increased surface of the conduit.

These two opposing phenomena indicate the existence of an optimal arch curve ( $D/2r$ ) with minimal flow loss. For a vessel with a 90-degree curve, the optimal value of  $D/2r$  is equal to 0.29. As the Reynolds number rises, so does

the velocity of the flow, which becomes more turbulent; the forces of inertia begin to prevail over viscosity forces, which, however, remain dominant near the aortic walls.

The curvature of the aortic arch and its diameter change with age [28]. Increased aortic stiffness results in a longer arch radius and aortic diameter. At the age of 30, the average radius of the aortic arch ( $r$ ) is approximately 68 mm, and the diameter of the ascending aorta ( $D$ ) is approximately 27.5 mm [28]. Above the age of 70, the aortic arch is enlarged to 83 mm on average, while the vascular diameter rises to 32.2 mm. As a result, in a normal aorta,

the Dean number (or rather the  $D/d$  diameter ratio) changes only slightly – by approximately 5% (from 0.4 to 0.38), irrespective of age. In the case of a pathologically dilated aorta, however, the  $D/d$  diameter ratio rises significantly. For the examined aortic models of normal structure, the ratio was 0.39, whereas, in the case of the model of a dilated aorta with BAV (model 2), the  $D/d$  ratio increased to 1.14. Repair surgery of the dilated aorta reduced the  $D/d$  diameter ratio to approximately 0.7.

The study results demonstrated that the distribution of velocities in the aorta is dependent on valve type and the shape of the aorta. The distribution of flow in an aorta of normal shape is typical for tricuspid valves. In the midsystolic phase, behind the valves, in the sinuses of Valsalva, a swirl can be observed that enables proper rinsing and adequate inflow into the coronary vessels during diastole. Flow stream through a TAV is central, with a characteristic flat velocity profile and a high velocity gradient in the boundary layer of the aorta.

The helical flow of blood through the aorta was observed in all models (Fig. 10), but in the case of the BAV models, the helical flow appeared earlier (immediately behind the valve), and its character was more complex, with increased secondary flow perpendicular to the aortic axis. This result fully confirms the image of flow through an aorta with BAV obtained from 4D MRI imaging of systolic flow [10]. The angle between the direction of the main stream flowing out of the valve during the mid-ejection phase and the surface of the external wall of the aortic arch depends on both the symmetry of valve cusp opening and the geometry of the ascending aorta. The larger the angle, the higher is the likelihood of changes in the mechanical properties of

the aortic walls (Fig. 11), resulting from increased pressure of the main stream on the wall of the aorta.

In the case of an already dilated aorta with BAV (model 2), this angle is nearly  $90^\circ$ ; the main stream collides with the outer wall of the aortic arch and divides into two streams, additional flow disturbances appear along with a clear area of stagnation (accumulation) (Fig. 12), in which flow velocity is reduced to zero, and static pressure takes the value of total pressure in accordance with the Bernoulli equation.

Another significant phenomenon that can be influenced by BAV is aortic wall deformation and dilatation. According to Wilton *et al.* [14], aortic dilatation most frequently occurs jointly with BAV; however, the size of the dilatation is independent of the degree of valve stenosis and results only from pathologies within the aortic wall.

The results of numerical simulations also confirm that the aortic deformation amplitude practically does not depend on valve type. Nonetheless, a significant influence of valve type on the spatial distribution of aortic wall deformations was observed.

In the case of BAV, aortic trunk deformation during systole is clearly unsymmetrical (Fig. 13). The asymmetry of deformations may be an additional factor causing aortic dilatation, that has not been taken into consideration before now. Girdauskas *et al.* [11] concluded that R-L cusp fusion is most frequently associated with aortic trunk dilatation, while R-N fusion is related to isolated dilatation of the ascending aorta (without dilating the aortic trunk). Computer simulations also confirm that the most significant deformation always occurs in the vicinity of the bulb and the inferior part of the ascending aorta – im-

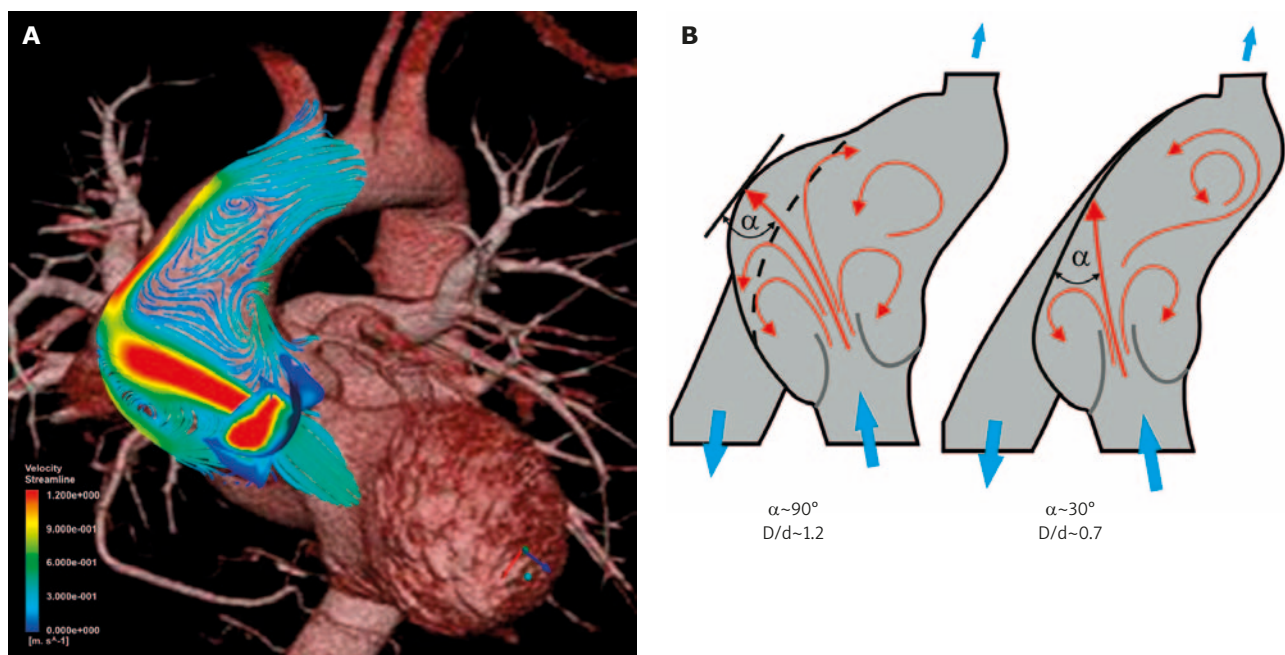


**Fig. 12A-B.** A) Lines of flow obtained from the computer simulation of a 65-year-old male patient with a dilated aorta and BAV. B) A scheme of the influence of aortic deformation on the angle between the direction of the main stream and the surface of the outer wall of the aortic arch at peak systole

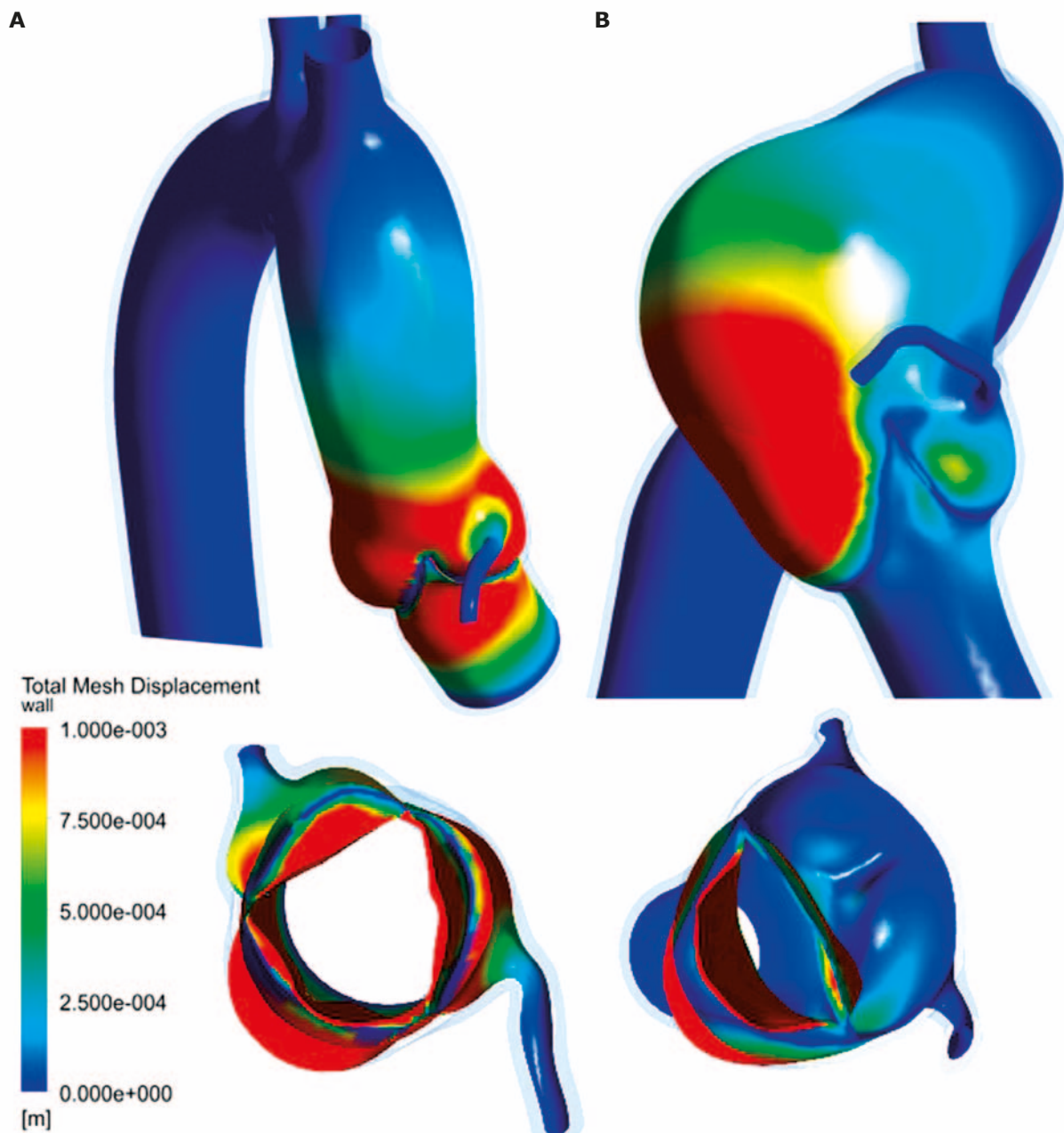


Fig. 13A-B. Deformation of the aorta and the valve cusps at mid-systole for selected models: A) model 1, B) model 2

mediately above the single non-coronary BAV cusp. Aortic deformation is pulsatile and synchronized with the cardiac cycle; moreover, it depends on valve cusp dynamics and retrograde swirls in the sinuses to a larger extent than on the velocity of the main stream flowing out of the valve. After many years of life, such a dynamic and unsymmetrical deformation may result in aortic wall fatigue and may significantly change the mechanical properties of the wall. The concept of elastin fatigue is based on the premise that the oscillations of the arterial wall cause a cyclical stretching of the elastin fibers and may result in the stiffening of the arterial walls due to the transfer of strain from elastin to collagen [29]. The loss of vascu-

lar compliance resulting from damage to the elastin layer and, thereby, the changes of the mechanical properties of the arterial wall play an important role in the regulation of blood pressure and the pathogenesis of arterial hypertension.

In the case of aortas with normal valves (model 1), maximum deformation (3 mm) occurs in the vicinity of the non-coronary sinus at mid-systole (0.4 s). However, in this case, the deformation of the wall of the ascending aorta is more symmetric than in the case of the remaining models of aortas with BAV.

The change of aortic geometry resulting from the replacement of the dilated part of the aorta impacts the dis-

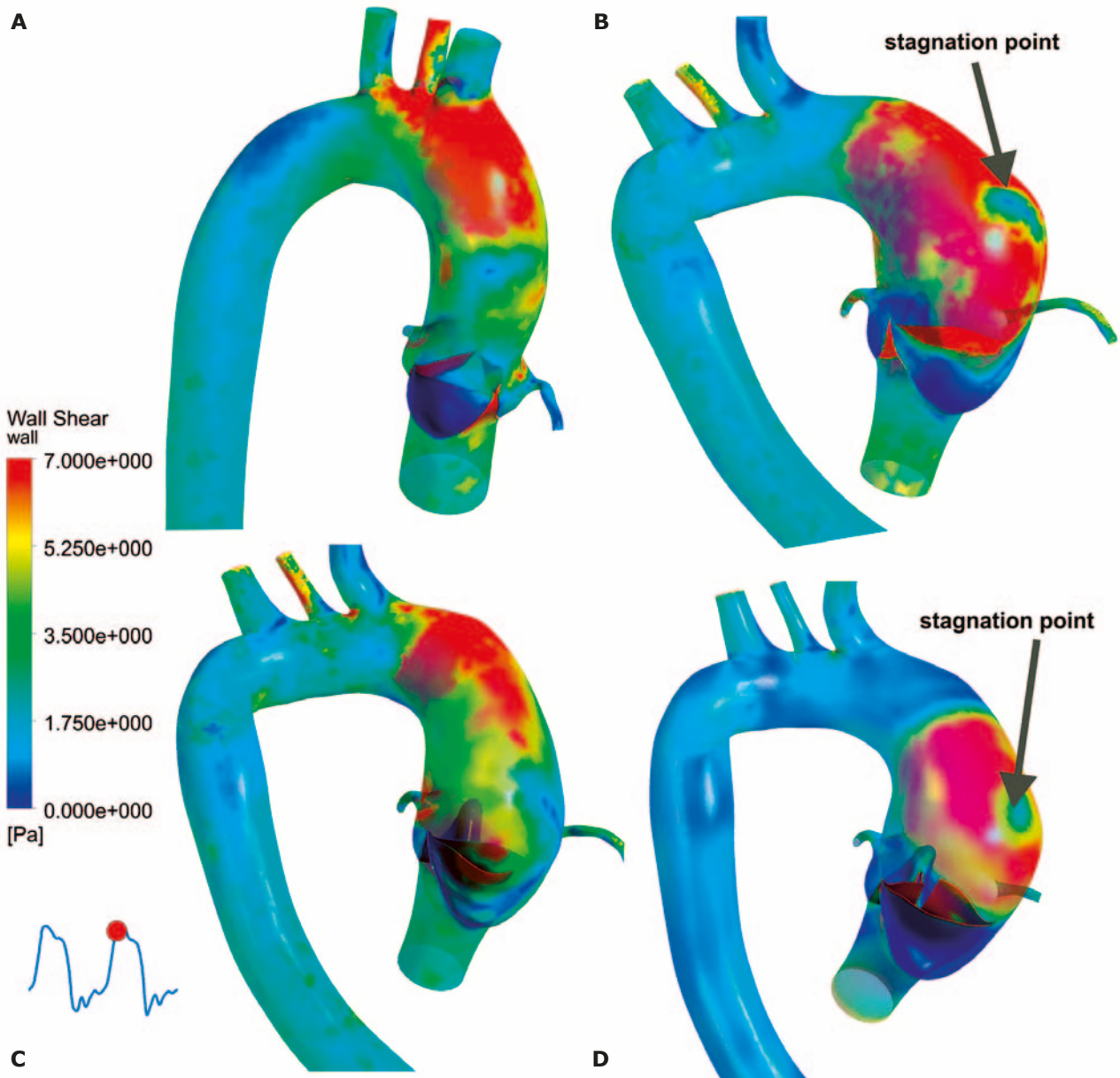
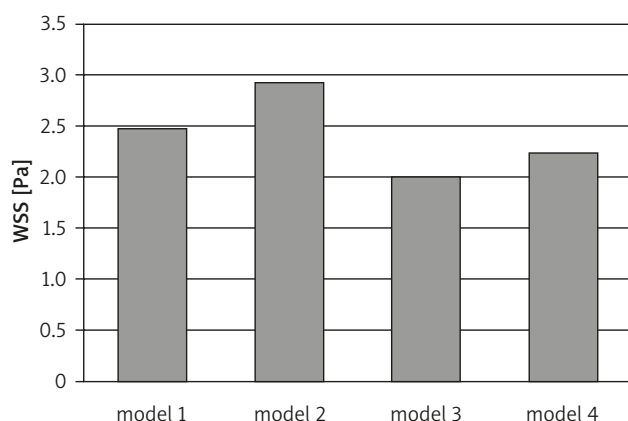


Fig. 14A-D. Distribution of aortic wall shear stresses at mid-systole in dependence on model type

tribution of aortic flow velocities and stresses (Fig. 10, Fig. 14). The flow accumulation area, characterized by high pressure and stress gradients, resulting from the collision of the main stream with the outer wall of the aortic arch and its division, disappears completely. A large swirling area appears (Fig. 10), which spreads throughout the area of the ascending aorta with an increased velocity component in the direction normal to the wall. As a result, maximum wall shear stresses appearing in the ascending aorta are approximately 80% lower than before the operation. The separation of the common BAV cusp increased the valve opening area during the ejection phase by only 5%; it also reduced the maximum valve flow velocity. Shear stresses and boundary stresses on the outer arch of the aorta were also minimally reduced. However, the primary characteristics of the flow did not change. A critical

area of flow stagnation, developing due to the stream division occurring on the outer wall of the aorta, could still be observed. Retrograde flow was also increased during valve closure (~16%) and diastolic leakage was revealed.

Increased wall shear stress values ( $WSS > 5$  Pa) are observed on the valve cusps, in the vicinity of the valve trunk, at the aortic sinotubular junction, and in the vicinity of the outer wall of the superior part of the ascending aorta (Fig. 14). Notwithstanding, small areas were observed in which instantaneous (1/100 s in duration) maximum stress values were much higher. In the vicinity of normal valve commissures, WSS reaches 154 Pa, whereas in the vicinity of BAV commissures, it is twice as high, reaching 308 Pa. In the ascending part of the aorta, the peak WSS value (91 Pa) was observed in model 2, in the vicinity of the RCCA inlet. However, mean WSS values



**Fig. 15.** The influence of geometry and valve type on the mean values of aortic wall shear stresses (WSS)

in all the models, during the whole cardiac cycle, did not exceed 3 Pa (Fig. 15) [30, 31].

Furthermore, bicuspid valves cause an increase of shear velocity by approximately 30%. In all models, high values of shear velocity (above 200 1/s) are observed primarily on the stream boundary near the valve cusps and between the main stream flowing out of the valve and the slow backflow in the sinuses.

## Conclusions

In the aorta, blood flow through the BAV generates asymmetric helical flow with a significant secondary flow and increased turbulence area. Asymmetric aortic wall deformation, as well as the increase and redistribution of stress, may constitute the primary reasons behind endothelial damage and aortic dissection in BAV patients.

Unsymmetrical stretching of elastin fibers may enhance the drop in vascular compliance due to the fatigue effect and elastin layer damage. Areas of congestion and high wall shear stress appear in the already dilated aorta.

The critical moment comes when, due to the pathological change of aortic geometry, the direction of the main blood stream generated by the valve becomes perpendicular to the outer wall of the aortic arch. An accumulation area, characterized by very high kinetic energy dissipation values, is created, which may consequently lead to endothelial dysfunction, aneurysm development, or aortic dissection.

In contrast to the separation of the common BAV cusp, the surgical repair of the geometry of a dilated aorta improves hemodynamic conditions in the ascending aorta, reduces wall stresses, and, most importantly, eliminates the critical area of accumulation on the outer wall of the ascending aorta.

*In vitro* modeling techniques allow for the individual evaluation of basic hemodynamic parameters. Two parameters may be particularly helpful in evaluating the risk of aortopathy (dilatation or dissection of the ascending part of the aorta) and determining the necessity of conducting preventive aortic valvuloplasty or replacing the ascend-

ing aorta with a prosthesis in BAV patients without overt hemodynamic defects: the Dean number and the angle between the direction of the main stream flowing out of the valve during the mid-ejection phase and the surface of the external wall of the aortic arch.

Analyzing a larger number of patients with bicuspid aortic valves will enable the empirical relations between the values of the abovementioned parameters to be determined in dependence on aortic deformation and stress. Therefore, *in vitro* modeling studies concerning aortic hemodynamics in varyingly dilated ascending aortas will be continued.

## Acknowledgements

The study was conducted as part of the N518 497239 research project of the Polish Ministry of Science and Higher Education.

The authors would also like to express their gratitude to M. Jakubowski and A. Klisowski for their technical support during the project.

## References

1. Siu SC, Silversides CK. Bicuspid aortic valve disease. *J Am Coll Cardiol* 2010; 25: 735-1097.
2. Abbott ME, Hamilton WF. Coarctation of the aorta of the adult type. *Am Heart J* 1928; 3: 381-421.
3. Bonderman D, Gharehbaghi-Schnell E, Wolleneck G, Maurer G, Baumgartner H, Lang IM. Mechanisms underlying aortic dilatation in congenital aortic valve malformation. *Circulation* 1999; 99: 2138-2143.
4. Hahn RT, Roman MJ, Mogtader AH, Devereux RB. Association of aortic dilation with regurgitant, stenotic and functionally normal bicuspid aortic valve. *J Am Coll Cardiol* 1992; 19: 283-288.
5. McKusick VA, Logue RB, Bahnson HT. Association of aortic valvular disease and cystic medial necrosis of the ascending aorta. Report of four cases. *Circulation* 1957; 16: 188-194.
6. Pachulski RT, Weinberg AL, Chan KL. Aortic aneurysm in patients with functionally normal or minimally stenotic bicuspid aortic valve. *Am J Cardiol* 1991; 67: 781-792.
7. Ward C. Clinical significance of the bicuspid aortic valve. *Heart* 2000; 83: 81-85.
8. Siniawski H. Active Infective Aortic Valve Endocarditis with Infection Extension. Clinical Features Perioperative Echocardiographics Findings and Results of Surgical Treatment. Steinkopff Verlag 2006.
9. Robicsek F, Thubrikar MJ, Cook JW, Fowler MD. The congenitally bicuspid aortic valve: how does it function? Why does it fail? *Ann Thorac Surg* 2004; 77: 177-185.
10. Hope MD, Hope TA, Meadows AK, Ordovas KG, Urbana TH, Alley MT, Higgins CB. Bicuspid aortic valve: four-dimensional MR evaluation of ascending aortic systolic flow patterns. *Radiology* 2010; 255: 53-61.
11. Girdauskas E, Borger M, Secknus M, Girdauskas G, Kuntze T. Is aortopathy in bicuspid aortic valve disease a congenital defect or a result of abnormal hemodynamics? A critical reappraisal of a one-sided argument. *Eur J Cardiothorac Surg* 2011; 6: 809-814.
12. Wilton E, Jahangiri M. Post-stenotic aortic dilatation. *J Cardiothorac Surg* 2006; 1: 1-11.
13. Cripe BC, Andelfinger G, Martin LJ, Shoener K, Woodrow D. Bicuspid aortic valve is heritable. *J Am Coll Cardiol* 2004; 44: 138-143.
14. Sabet HY, Edwards WD, Tazelaar HD, Daly RC. Congenitally bicuspid aortic valves: a surgical pathology study of 542 cases (1991 through 1996) and a literature review of 2715 additional cases. *Mayo Clin Proc* 1999; 74: 14-26.
15. Campbell M. Calcific aortic stenosis and congenital bicuspid aortic valves. *Br Heart J* 1968; 30: 606-616.
16. David TE. Surgical treatment of ascending aorta and aortic root aneurysms. *Prog Cardiovasc Dis* 2010; 52: 438-444.



17. Pettersson GB, Crucean AC, Savage R, Halley CM, Grimm RA, Svensson LG, Naficy S, Gillinov AM, Feng J, Blackstone EH. Toward predictable repair of regurgitant aortic valves: a systematic morphology-directed approach to bicommissural repair. *J Am Coll Cardiol* 2008; 52: 40-49.
18. Lei M, Kleinstreuer C, Archie JP. Hemodynamic simulations and computer-aided designs of graft-artery junctions. *J Biomech Eng* 1997; 119: 343-348.
19. Malota Z, Nawrat Z, Kostka P, Mizerski J, Nowiński K, Waniewski J. Physical and computer modelling of blood flow in a systemic-to-pulmonary shunt. *Int J Artif Organs* 2004; 27: 990-999.
20. Weinberg E, Mofrad MR. A multiscale computational comparison of the bicuspid and tricuspid aortic valves in relation to calcific aortic stenosis. *J Biomech* 2008; 41: 3482-3487.
21. Chandran KB, Vigmostad SC. Patient-specific bicuspid valve dynamics: overview of methods and challenges. *J Biomech* 2013; 46: 208-216.
22. Vesely I. Heart valve tissue engineering. *Circ Res* 2005; 97: 743-755.
23. Menter FR. Two-equation eddy-viscosity turbulence models for engineering applications. *AIAA Journal* 1994; 32: 1598-1605.
24. Lantz J, Renner J, Karlsson M. Wall shear stress in a subject specific human aorta – Influence of fluid-structure interaction. *Int J Appl Mech* 2011; 4: 759-778.
25. Waite L, Jerry Fine PE. *Applied Biofluid Mechanics*. McGraw-Hill Companies, Inc. 2007.
26. Reul H. Hydraulic analog model of the systemic circulation. *Advanced in Cardiovascular Physics* 1983; 5: 43-54.
27. Ku DN. Blood flow in arteries. *Annu Rev Fluid Mech* 1997; 29: 399-434.
28. Redheui A, Yu W, Mousseaux E, Harouni AA, Kachenoura N, Wu CO, Bluemke D, Lima JA. Age-related changes in aortic arch geometry: relationship with proximal aortic function and left ventricular mass and remodeling. *J Am Coll Cardiol* 2011; 58: 1262-1270.
29. Fedak PW, Verma S, David TE, Weisel RL, Butany J. Clinical and pathophysiological implications of a bicuspid aortic valve. *Circulation* 2002; 106: 900-904.
30. Nandy S, Tarbell JM. Flush mounted hot film anemometer measurement of wall shear stress distal to a tri-leaflet valve for Newtonian and non-Newtonian blood analog fluids. *Biorheology* 1987; 24: 483-500.
31. Weston MW, LaBorde DV, Yoganathan AP. Estimation of the shear stress on the surface of an aortic valve leaflet. *Ann Biomed Eng* 1999; 27: 572-579.